Modelling and Imaging within the Diffraction Limit with Application in Engineering Geophysics

L.-J. Gelius, H. Westerdahl, and F.N. Kong
Norwegian Geotechnical Institute, P.O.Box 3930 Ullevaal Hageby, N-0806 Oslo, Norway

SUMMARY

In engineering geophysics the task is often to locate and/or image different buried objects or structures. If we consider geotechnical investigations typically targets will be cavities, buried drums, tunnels, pipelines and rock pieces in soil. Correspondingly, in non-destructive testing we aim to characterize structural distortions or to image target objects embedded in a given structure.
In this paper we will consider the problem of object localization and structure characterization for such applications. Moreover, we assume that the probing wavelengths are close to the characteristic dimensions of the various targets, which implies that diffracted energy will be of great importance.
Methods for modelling and imaging within the diffraction limit are presented, which are valid for both acoustic and radar waves. A sample of controlled field data examples will be presented to illustrate the methods.

MODELLING BASED ON ANALYTICAL SOLUTIONS

We recognize that in many cases in engineering geophysics the target objects can be approximated by simple objects like circular or elliptical cylinders and liners in 2-D or spheres in 3-D. Hence, we have developed a number of modelling programs based on exact analytical solutions for such reference objects [1]. These solutions are fast when compared with finite-element computations, and also far more stable for cases where the probing wavelengths are close to the characteristic dimensions of the target.
As an example, let us now present results employing an exact solution for elastic scattering from a liner. Fig.1 shows the synthetic test model involving a concrete tube embedded in a slime material ($v_p = 1600m/s, v_s = 600m/s$). Corresponding data are given in Fig.2 employing a centered surface source ($f = 2000Hz$) and five different receiver positions at the same surface. We can easily identify the scattered p- and s-waves.

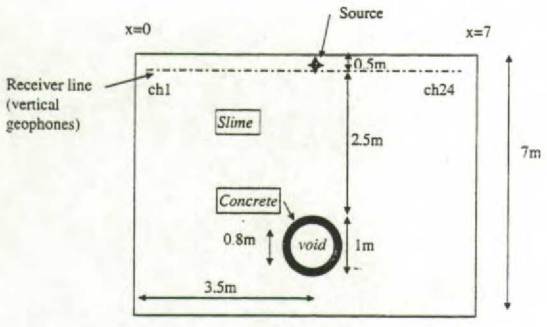

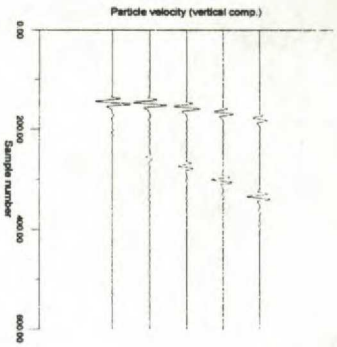

FIG. 1 Test model

FIG.2 Synthetic data corresponding to model in Fig.1

OBJECT LOCALIZATION

We consider the problem of computing the most probable location of a target based on surface measurements (radar or acoustics). Our algorithm makes use of the maximum likelihood estimator (MLE), which represents a correlation between the measured data and synthetic data generated for the object of interest at different locations. The MLE can be written explicitly as [2]

$$\xi_N(\vec{r}_c) = \frac{\mathrm{Re}\int D(\vec{\eta})d'^{*}(\vec{\eta},\vec{r}_c)d\vec{\eta}}{\sqrt{\int D(\vec{\eta})D^{*}(\vec{\eta})d\vec{\eta}\cdot\int d'(\vec{\eta},\vec{r}_c)d'^{*}(\vec{\eta},\vec{r}_c)d\vec{\eta}}} \tag{1}$$

where $\vec{\eta}$ is a generalized coordinate vector, D denotes the surface measurements and d' is the data template (i.e. synthetic data corresponding to an object at position $\vec{r}_c$).

We have carried out a controlled field experiment where the target object was a drum made of steel. The drum was air-filled and embedded in dry sand, as shown in Fig.3. The diameter of the object was 0.6m, and the distance from the surface to the top of it was 2.0m. Surface data were acquired along a line perpendicular to the symmetry-axis of the drum and running symmetrically across the object. We employed a GPR system (step-frequency based) developed by the Norwegian Geotechnical Institute (NGI) [3] to acquire the data. In the experiment considered here, we wanted the wavelength to be in the order of 1m which is close to the characteristic dimensions of the target object. Since the radar velocity in sand was found to be close to 20cm/ns, a wavelength of 1m corresponded to a frequency of 200MHz. Hence, we used a 0.5m dipole antenna covering a frequency band from 1MHz to 400MHz. Moreover, we collected data employing a bistatic configuration, i.e. a constant transmitter-receiver offset of 1m. A total number of 59 measurements were carried out, in increments of 0.1m, and covering a total distance of 5.8m (symmetrically around the target object).

The coordinate vector $\vec{\eta}$ now contains two parameters, i.e.

$$\vec{\eta} = \{x_h, \omega\} \tag{2}$$

where x_h is the mid-point coordinate and ω is the angular frequency. If we assume a strong-scattering target object which is small in number of wavelengths, the data template d' in Eq.(1) can be written explicitly as [2]

$$d'(x_h,\omega,\vec{r}_c)=\frac{2i}{R_{sc}R_{gc}}\frac{\sqrt{\pi\omega i(R_{sc}+R_{gc}+R_{hc}^2-h^2/4)}}{\sqrt{c_0(R_{sc}+R_{gc})}}\cdot\exp\left[i\omega(R_{sc}+R_{gc})/c_0\right] \qquad (3)$$

where $R_{sc}, R_{gc}, and\ R_{hc}$ are the distances from the transmitter, the receiver and the midpoint, respectively, to the center of the object. The parameter h in Eq.(3) is the fixed transmitter-receiver offset and c_0 is the uniform background velocity. By combining Eqs.(1) and (3) we finally obtain the MLE used in this study. Fig.4 shows the result obtained applying these formulae, i.e. a contour-plot of the 2-D matrix representing the estimator. The depth range is from the surface down to 4m, and the spatial sampling interval used in the computations was 0.1m. We can see from Fig.4 that the method locates the target object at the correct depth but slightly shifted to the left. The reason for this shift is probably due to an inaccurate background velocity field (assumed to be uniform here).

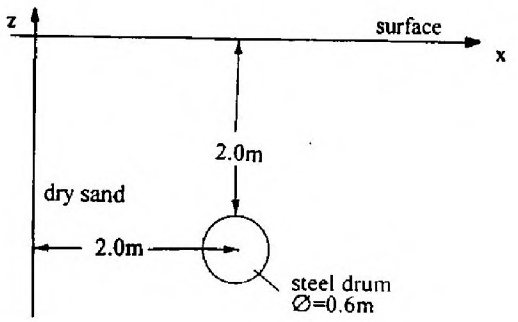

FIG.3 Schematics of test site

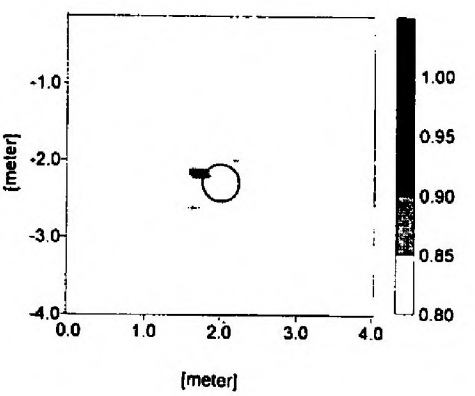

FIG.4 The computed MLE based on radar data

STRUCTURE CHARACTERIZATION

Once more we assume fixed-offset surface measurements collected along a line. We now consider the task of computing a structural image based on recordings of diffracted wave energies. We assume 2.5-D data (i.e. 3-D wavepropagation in a 2-D model) and a uniform background. Moreover, we consider the scalar case only. Based on the generalized Radon transform [4], which takes into account that the diffracted waves deviate from straight lines, we arrive at the following reconstruction algorithm (where $\hat{\xi}$ is a generalized reflectivity function)

$$\hat{\xi}(x,z)=\frac{2z}{c_0\sqrt{\pi c_0}}\int d(x_h,t=\tau)\sqrt{(R_s+R_g)R_sR_g}\cdot\left[\frac{1}{R_s^2}+\frac{1}{R_g^2}\right]\cdot\sqrt{1+\frac{(R_h^2-h^2/4)}{R_sR_g}}dx_h \qquad (4)$$

where $R_s, R_g\ and\ R_h$ are the distances from the transmitter, the receiver and the mid-point, respectively, to an image point (x,z), and d is the measurement data after wavelet

deconvolution and 'differentiation' filtering (transfer function $\sqrt{i\omega}$). The imaging time τ in Eq.(4) is defined as

$$\tau = (R_s + R_g) / c_0 \tag{5}$$

We will now present results obtained employing this method in connection with radar measurements in concrete (non-destructive testing). The test sample was a concrete block with a length of 1m and a vertical thickness of 0.15m. The target objects were five tendons (diameter of 0.05m), and radar data were acquired at 159 different positions along a surface profile. We used a radar system developed by NGI based on two horn antennas placed 0.03m apart. The size of each antenna was 0.06m x 0.05m, and the frequency band covered was from 1.0 to 6.0GHz. The lower part of Fig.5 shows the final reconstruction obtained. Since the objects are strong we will only obtain images of the upper boundary of each tendon. We can easily identify four out of five original targets, but tendon number two is not visible. The reason for this result is probably due to interference from the rebars which are laying above. But all in all, the result in Fig.5 is acceptable and shows that the method works well.

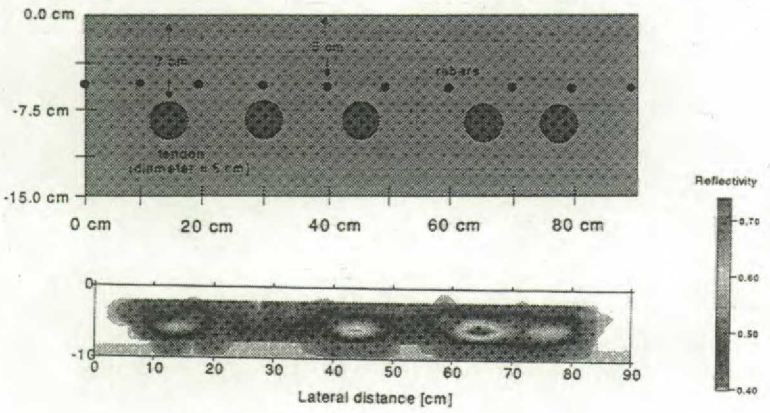

FIG. 5 NDT example

CONCLUDING REMARKS

We have employed the principle of frequency tuning, which assumes that the medium wavelength associated with the source field is comparable to the characteristic dimensions of the target object(s). Within this formulation we have presented valid methods for both modelling, object localization and structure characterization.

REFERENCES

[1] Pao, Y.H. and Mow, C.C., 1973: Diffraction of elastic waves and dynamic stress concentrations. A Rand Corporation Research Study. Russak and Company Inc., New York

[2] Gelius, L.-J., 1996: EM target location. Geophys.Prosp. **44**, 479-494.

[3] Kong, F.N. and By, T.L., 1995: Performance of a GPR system which uses step frequency signals. J. Appl. Geoph. **33**, 15-26.

[4] Beylkin, G.,1985: Imaging of discontinuities in the inverse scattering problem by inversion of a causal generalized Radon transform. Journal of Mathematical Physics **26**, 99-108.